

# HaluNet: Multi-Granular Uncertainty Modeling for Efficient Hallucination Detection in LLM Question Answering

Chaodong Tong<sup>1,2</sup>, Qi Zhang<sup>3</sup>, Jiayang Gao<sup>4</sup>, Lei Jiang<sup>1</sup>, Yanbing Liu<sup>1,2</sup>, and Nannan Sun<sup>1\*,2</sup>

<sup>1</sup>Institute of Information Engineering, Chinese Academy of Sciences, Beijing, China

<sup>2</sup>School of Cyber Security, University of Chinese Academy of Sciences, Beijing, China  
 {tongchaodong, jianglei, liyanbing, sunnannan}@iie.ac.cn

<sup>3</sup>China Industrial Control Systems Cyber Emergency Response Team, Beijing, China  
 bonniezhangqi@126.com

<sup>4</sup>Beijing Institute of Computer Technology and Application, Beijing, China  
 nemo830218@gmail.com

**Abstract.** Large Language Models (LLMs) excel at question answering (QA) but often generate hallucinations, including factual errors or fabricated content. Detecting hallucinations from internal uncertainty signals is attractive due to its scalability and independence from external resources. Existing methods often aim to accurately capture a single type of uncertainty while overlooking the complementarity among different sources, particularly between token-level probability uncertainty and the uncertainty conveyed by internal semantic representations, which provide complementary views on model reliability. We present **HaluNet**, a lightweight and trainable neural framework that integrates multi granular token level uncertainties by combining semantic embeddings with probabilistic confidence and distributional uncertainty. Its multi branch architecture adaptively fuses what the model knows with the uncertainty expressed in its outputs, enabling efficient one pass hallucination detection. Experiments on SQuAD, TriviaQA, and Natural Questions show that HaluNet delivers strong detection performance and favorable computational efficiency, with or without access to context, highlighting its potential for real time hallucination detection in LLM based QA systems.

**Keywords:** Large Language Models · Question Answering · Hallucination Detection · Token-Level Signals · Multi-Granular Uncertainty

## 1 Introduction

Question answering (QA) is a core capability of modern large language models (LLMs), powering applications from search engines to conversational assistants and autonomous LLM agents. While LLMs achieve strong performance on open-domain QA [12, 24, 30], they often produce hallucinations in the form of factual errors or fabricated content, which compromise reliability [4, 12]. Traditional detection methods relying on external knowledge bases or multi-step verification

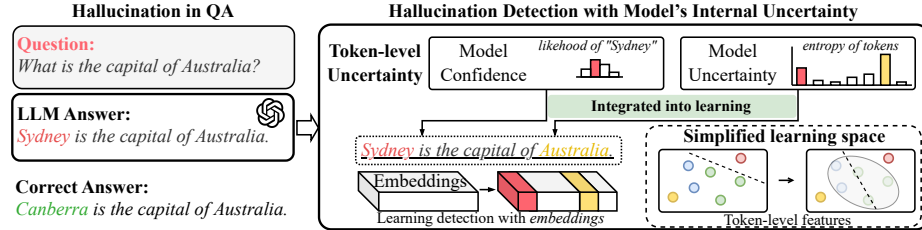


Fig. 1: Integrating token-level uncertainty signals simplifies and enhances the learning process for hallucination detection.

are computationally costly, difficult to deploy in real time, and limited by knowledge coverage [3,5,26].

Recent studies have explored detecting hallucinations via internal model uncertainty, broadly categorized as epistemic uncertainty, reflecting gaps in model knowledge, and aleatoric uncertainty, arising from ambiguous or underspecified contexts [11,25]. These uncertainties manifest in token probabilities, hidden states, and output variability [6,13]. Probability-based methods estimate token-level confidence using likelihoods or entropy, effectively capturing aleatoric uncertainty [18,29,1]. Representation-based methods analyze embeddings to capture epistemic uncertainty [6,28,8]. Complementarily, semantic-consistency methods, which can partially reflect both types of uncertainty, evaluate agreement across multiple generated outputs [15,19,4]. However, they incur substantial computational cost and often struggle to provide accurate uncertainty estimates [25]. Some studies attempt to combine multiple features [2,17,27], but these approaches typically cover only part of the uncertainty spectrum and often treat signals independently, limiting robust hallucination detection.

Even when multiple features are combined, obtaining effective supervision to fully leverage them remains challenging. Human-annotated hallucination labels can provide high-quality supervision, but they are costly and difficult to scale [18,12]. To mitigate this issue, some methods explore model-driven or automated supervision signals [19,20,4,7]. For example, approaches such as semantic entropy and SelfCheckGPT [4,19] employ an LLM-as-a-Judge paradigm to generate model-driven supervision signals; however, these methods typically use the resulting signals, i.e., pseudo-gold labels, only for evaluation. Research has shown that, despite their simple and low-cost generation, these pseudo-gold labels often exhibit high consistency across multiple generations, making them a useful proxy in certain evaluation scenarios [25].

To address these limitations, we propose **HaluNet**, a lightweight framework that unifies multiple token-level uncertainty signals (Fig. 1). HaluNet employs a multi-branch design to jointly model semantic embeddings, token log-likelihoods, and predictive entropy, and fuses these signals via attention or an MLP to capture cross-signal interactions efficiently. Training is supervised by LLM-as-a-Judge signals, providing scalable supervision without manual annotation and

enabling accurate hallucination detection in both context-rich and context-free settings.

Our contributions are summarized as follows:

- We present **HaluNet**, a unified uncertainty fusion framework that integrates semantic, probabilistic, and distributional signals from a single LLM generation.
- We develop a lightweight training paradigm that enables robust hallucination detection with or without external context, eliminating the need for costly human annotations.
- We demonstrate state-of-the-art (SOTA) performance across diverse QA benchmarks, highlighting both strong generalization and high computational efficiency.

## 2 Related Work

Recent work leverages internal model uncertainty signals to detect hallucinations in LLM outputs. **Probability-based methods** estimate aleatoric uncertainty using token likelihoods or entropy, with low-probability tokens often indicating errors [1,18,29,21]. While efficient, these methods may fail to capture dependencies reflected in semantic or epistemic signals.

**Representation-based approaches** analyze hidden states, attention, or embeddings to capture epistemic uncertainty, revealing how confidently a model encodes factual information [6,8,28]. They capture global semantic reliability but often require heuristic layer choices or task-specific probes [13,23].

**Semantic consistency methods** assess output stability under sampling or perturbation [4,15,19]. These methods partially reflect both aleatoric and epistemic uncertainty, but repeated sampling is costly and limits scalability.

**Hybrid or supervised approaches** integrate multiple features such as attention dynamics, embeddings, and token probabilities [2,17,27,28]. They improve detection accuracy but often rely on large annotated datasets or loosely coupled feature fusion, limiting scalability.

In contrast, **HaluNet** unifies probabilistic, distributional, and semantic signals in a single framework, enabling efficient cross-signal fusion and reduced supervision requirements.

## 3 Methodology

### 3.1 Problem Definition

We study **answer-level hallucination detection**, predicting whether an answer  $a$  to a question  $q$  (optionally with context  $c$ ) is hallucinatory. Given a language model  $\mathcal{M}_\theta$  generating  $a = (x_1, \dots, x_L)$ , the goal is to learn a detector  $f_\phi$  mapping  $(q, c, a; \mathcal{M}_\theta) \mapsto [0, 1]$ , where higher scores indicate higher hallucination likelihood. The model is trained on  $\mathcal{D} = \{(q_i, c_i, a_i, y_i)\}_{i=1}^N$  with  $y_i \in \{0, 1\}$ ,

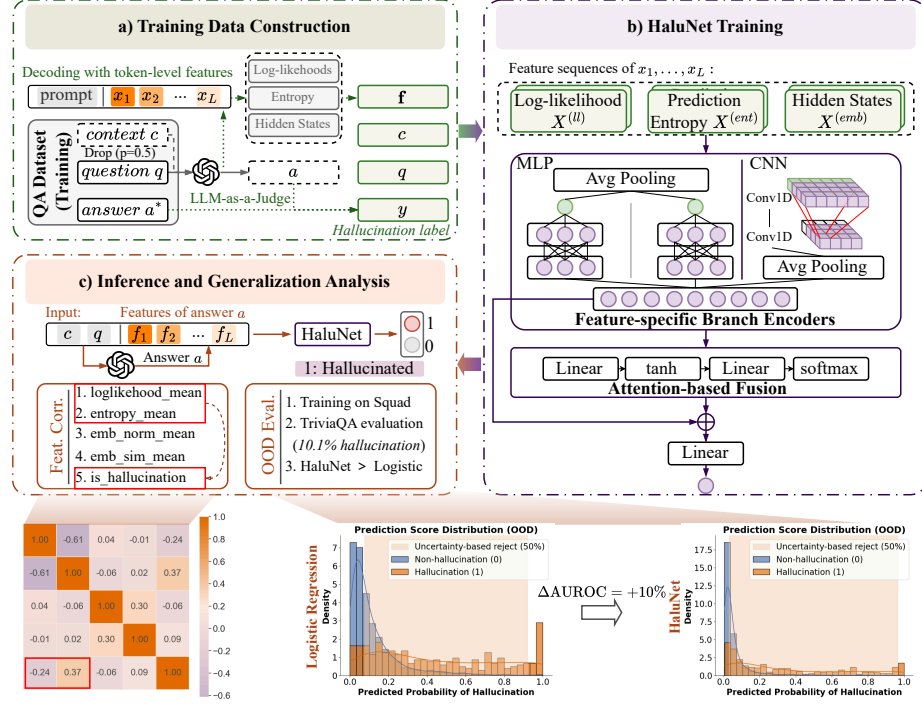


Fig. 2: HaluNet workflow: (a) training data construction, (b) multi-branch feature extraction and fusion, (c) inference and generalization analysis for robust hallucination detection.

where  $y_i = 1$  indicates a hallucinatory answer and  $y_i = 0$  a factual one. Following prior work [4,25], labels are obtained by sampling low-temperature answers per question and evaluating them via an **LLM-as-a-Judge** framework [4,6,7,25].

### 3.2 Training Data Construction

Starting from QA datasets with tuples  $(c, q, a^*)$ , where  $c$  is optional context,  $q$  the question, and  $a^*$  the reference answer, we construct training instances  $(c, q, a, f, y)$  (Fig. 2a). Here,  $a$  is a low-temperature ( $T = 0.1$ ) model-generated answer,  $f$  contains token-level features including log-likelihoods, entropies, and embeddings (Section 3.3), and  $y$  is the hallucination label from an **LLM-as-a-Judge** framework. To capture context-dependent uncertainty, each question is paired with its full context  $c$  with probability 0.5, balancing hallucinated and faithful examples for stable training.

### 3.3 Feature Extraction

HaluNet captures token-level generation uncertainty from  $\mathcal{M}_\theta$  via three complementary signals: log-likelihoods, entropies, and hidden states, jointly modeling

predictions and uncertainty. For token  $x_t$  with preceding tokens  $x < t$ , probabilistic confidence is  $\ell_t = \log p_{\mathcal{M}_\theta}(x_t \mid x < t, q, c)$ , while distributional uncertainty is  $H_t = -\sum_{v \in V} p_{\mathcal{M}_\theta}(v \mid x < t, q, c) \log p_{\mathcal{M}_\theta}(v \mid x < t, q, c)$ . Semantic trajectory is encoded as  $\mathbf{h}_t = \text{HiddenState}_{\mathcal{M}_\theta}^{(l)}(x_t \mid x_{<t}) \in \mathbb{R}^d$ . Each instance is represented as  $(c, q, \mathbf{L}, \mathbf{H}, \mathbf{E}, y)$ , where  $\mathbf{L}, \mathbf{H} \in \mathbb{R}^L$  are log-likelihood and entropy vectors, and  $\mathbf{E} \in \mathbb{R}^{L \times d}$  contains hidden embeddings (zero-padded to  $L = 50$ ), enabling cross-signal interaction learning.

### 3.4 HaluNet: Unified Hallucination Detection Network

We propose **HaluNet**, a lightweight network for hallucination detection operating on token-level features extracted from generated sequences (Fig. 2b). Let  $F = 3$  denote feature types: log-likelihoods, entropies, and hidden-state embeddings, with inputs  $\mathbf{X}^{(f)} \in \mathbb{R}^{L \times d_f}$ ,  $f = 1, \dots, F$  ( $\mathbf{X}^{(1)} = \mathbf{X}^{(\text{ll})}$ ,  $\mathbf{X}^{(2)} = \mathbf{X}^{(\text{ent})}$ ,  $\mathbf{X}^{(3)} = \mathbf{X}^{(\text{emb})}$ ). Each branch  $B_f$  produces a latent vector  $\mathbf{h}^{(f)} \in \mathbb{R}^{d_h}$ .

For scalar features ( $d_f = 1$ ), we apply mean pooling followed by a two-layer MLP:

$$\mathbf{h}^{(f)} = \text{MLP}\left(\frac{1}{L} \sum_{t=1}^L \mathbf{X}_t^{(f)}\right). \quad (1)$$

For embedding features ( $d_f = d_{\text{emb}}$ ), a two-layer 1D convolution with kernel size 3 and padding 1 is applied, followed by ReLU activations and adaptive average pooling:

$$\mathbf{h}^{(f)} = \text{AvgPool1d}\left(\text{ReLU}(\text{Conv}_2(\text{ReLU}(\text{Conv}_1(\mathbf{X}^{(f)}))))\right). \quad (2)$$

Branch outputs are stacked:

$$H = [\mathbf{h}^{(1)}, \dots, \mathbf{h}^{(F)}] \in \mathbb{R}^{F \times d_h}, \quad (3)$$

and fused either via attention:

$$\alpha^{(f)} = \frac{\exp(\mathbf{w}^\top \tanh(W_a \mathbf{h}^{(f)}))}{\sum_{f'} \exp(\mathbf{w}^\top \tanh(W_a \mathbf{h}^{(f')}))}, \quad \mathbf{h}_{\text{fused}} = \sum_f \alpha^{(f)} \mathbf{h}^{(f)}, \quad (4)$$

or by concatenation:

$$\mathbf{h}_{\text{fused}} = \text{MLP}([\mathbf{h}^{(1)}; \dots; \mathbf{h}^{(F)}]). \quad (5)$$

The fused vector is projected to a logit:

$$\hat{s} = \mathbf{w}_o^\top \mathbf{h}_{\text{fused}} + b_o, \quad (6)$$

and trained with binary cross-entropy:

$$\mathcal{L}_{\text{BCE}} = -[y \log \sigma(\hat{s}) + (1 - y) \log(1 - \sigma(\hat{s}))]. \quad (7)$$

At inference, the hallucination probability is

$$p = \sigma(\hat{s}), \quad \hat{y} = \mathbb{1}\{p \geq 0.5\}, \quad (8)$$

while  $p$  or  $\hat{s}$  can be used as a continuous score for ranking metrics.

HaluNet captures complementary aspects of generation uncertainty. Log-likelihoods and entropies measure probabilistic confidence and local uncertainty, while embeddings encode the semantic trajectory of the sequence. Multi-branch encoders allow each feature type to leverage the most appropriate architecture, with adaptive fusion balancing efficiency and expressiveness. The effectiveness of the features and the rationale of the HaluNet architecture are preliminarily validated in Fig. 2c.

## 4 Experiments

### 4.1 Setup

**Datasets.** We evaluate HaluNet on three QA benchmarks: **SQuAD** [22], **TriviaQA** [14], and **NQ-Open (NQ)** [16]. Each training set contains 10K answerable samples (TriviaQA split 8:2 for training and test), with SQuAD and TriviaQA containing equal proportions of context-present and context-free instances, while NQ is fully context-free (statistics shown in Table 1). The **context ratio (CR)** controls the proportion of contextual inputs (**CR=1**: context-present, **CR=0**: context-free). All samples are labeled using the LLM-as-a-Judge framework [4,6,7]. We assess both **in-distribution (ID)** performance under varying CRs and **out-of-distribution (OOD)** transfer across datasets.

Table 1: Dataset sizes and hallucination rates (%) for sampled QA datasets under different context ratios.

Dataset	Ori. (train/test)	Sampl. (train/test)	Hallu. (train / CR0 / CR1)
<i>SQuAD</i>			
Llama3-8B	130k / 11.9k	10k / 5.9k	41.7 / 82.4 / 17.1
Qwen3-14B	130k / 11.9k	10k / 5.9k	43.4 / 74.7 / 8.6
<i>TriviaQA</i>			
Llama3-8B	12.3k / 3.1k	10k / 3.1k	19.6 / 29.8 / 10.1
Qwen3-14B	12.3k / 3.1k	10k / 3.1k	41.8 / 42.4 / 15.6
<i>NQ</i>			
Llama3-8B	87.9k / 3.6k	10k / 3.6k	57.8 / 61.4 / -
Qwen3-14B	87.9k / 3.6k	10k / 3.6k	71.1 / 71.6 / -

**Implementation Details and Baselines.** In all experiments except for the architectural ablation study, we use a unified HaluNet configuration where all feature types are enabled, each branch is encoded with a CNN, and an MLP-based fusion module produces the final prediction. For Llama3-8B and Qwen3-14B, we extract token-level features including log likelihood, entropy, and hidden states from layer  $l = 20$  (Section 4.4). Each branch uses a CNN with  $d_{\text{conv}} = 64$  channels, kernel size 3, and padding 1, generating a  $d_h = 64$  representation. The fusion module is a two-layer MLP with a hidden size of  $d_{\text{mlp}} = 64$ . Models are trained with AdamW (learning rate  $1 \times 10^{-4}$ , batch size 32) for up to 20 epochs with early stopping based on validation AUROC.

Table 2: ID results under **CR=1**. Best and second-best scores are shown in bold and underlined. Latency denotes average inference time per 100 samples (s). Cell colors: green (sub-sec), yellow (sec-level), red (slow).

		SQuAD				TriviaQA				Latency /100 (s)					
		ROC		RAC		F1@B		RA@50		ROC	RAC	F1@B	RA@50	Sample	Infer
		PE	0.732	<u>0.898</u>	0.427	0.934	0.723	0.913	0.394	0.952	105.435	0.001			
Llama3-8B	T-NLL	0.628	<u>0.854</u>	0.347	0.868	0.578	0.908	0.214	0.924	80.780	0.001				
	EmbVar	0.757	0.887	0.468	0.939	0.781	0.945	0.378	0.973	727.163	0.109				
	SE	0.619	0.849	0.346	0.859	0.766	0.948	0.409	0.967	743.258	29.927				
	SEU	0.763	0.079	0.457	0.061	0.827	0.030	0.457	0.023	731.105	2.068				
	SelfCheckGPT	0.772	0.878	0.466	<u>0.944</u>	0.779	0.934	0.356	<u>0.978</u>	760.002	87.161				
	$P(\text{True})$	0.692	0.878	0.398	0.903	0.819	0.962	0.415	<u>0.978</u>	81.557	30.413				
	Logistic	0.735	0.885	<u>0.488</u>	0.904	<u>0.848</u>	0.930	<u>0.577</u>	0.955	98.849	0.028				
	HaluNet (Ours)	<b>0.839</b>	<b>0.941</b>	<b>0.532</b>	<b>0.965</b>	<b>0.893</b>	<b>0.977</b>	<b>0.601</b>	<b>0.984</b>	97.663	0.124				
Qwen3-14B	PE	0.705	0.938	0.274	0.961	0.719	0.900	0.361	0.920	127.035	0.001				
	T-NLL	0.577	0.947	0.130	0.956	0.589	0.176	0.332	0.173	131.44	0.001				
	EmbVar	0.726	0.957	0.308	<u>0.976</u>	0.744	0.863	0.490	0.912	1289.101	0.126				
	SE	0.665	0.956	0.278	0.968	0.750	0.880	0.542	0.904	1253.741	24.100				
	SEU	<u>0.748</u>	0.024	0.356	0.023	0.763	0.107	0.536	0.087	1302.565	1.948				
	SelfCheckGPT	0.652	0.956	0.371	0.966	0.774	0.884	0.588	0.907	1267.408	74.015				
	$P(\text{True})$	<u>0.748</u>	<b>0.970</b>	0.292	<b>0.985</b>	<u>0.891</u>	<u>0.937</u>	<b>0.727</b>	<b>0.961</b>	118.871	53.593				
	Logistic	0.699	0.924	0.322	0.943	0.794	0.926	0.558	0.937	121.403	0.042				
	HaluNet (Ours)	<b>0.781</b>	<u>0.961</u>	<b>0.393</b>	0.971	<u>0.856</u>	<b>0.948</b>	<u>0.665</u>	<u>0.960</u>	128.006	0.119				

HaluNet is compared with several representative uncertainty-based baselines. Probability-based baselines include **Predictive Entropy (PE)** [10] and **Token Negative Log-Likelihood (T-NLL)** [29]. Latent-space baselines measure embedding stability, e.g., **Embedding Variance (EmbVar)** and **Semantic Embedding Uncertainty (SEU)** [6]. Semantic-level baselines assess output consistency, including **Semantic Entropy (SE)** [4], **SelfCheckGPT** [19], and prediction-based  $P(\text{True})$  [4]. A **Logistic Regression** [9] classifier trained on our dataset serves as a supervised reference.

**Evaluation Metrics.** We evaluate hallucination detection using four metrics: **ROC** (AUROC), **RAC** (AURAC), **RA@50**, and **F1@B**. AUROC measures the ability to rank hallucinated versus non-hallucinated samples. RA@50 reports ac-

curacy on the top 50% most certain predictions, while AURAC integrates accuracy across all rejection thresholds. F1@B gives the maximum F1 over thresholds. For supervised methods, a fixed threshold of 0.5 is used, with predictions near 0.5 considered more uncertain. For unsupervised methods, scores are normalized so that higher values indicate higher uncertainty. Together, these metrics provide a comprehensive assessment of ranking, selective reliability, and overall hallucination detection performance.

## 4.2 In-Distribution Evaluation

Most prior work evaluates hallucination detection without context [4,6,29]. We additionally consider full-context inputs, summarized alongside no-context results in Tables 2 and 3.

Table 3: ID results under **CR = 0**.

	SQuAD				TriviaQA				NQ				
	ROC	RAC	F1@B	RA@50	ROC	RAC	F1@B	RA@50	ROC	RAC	F1@B	RA@50	
Llama3-8B	PE	0.710	0.694	0.898	0.746	0.711	0.805	0.512	0.841	0.663	0.480	0.765	0.521
	T-NLL	0.640	0.762	0.901	0.752	0.618	0.758	0.437	0.772	0.606	0.562	0.781	0.562
	EmbVar	0.724	0.730	0.903	0.750	0.833	0.857	0.628	0.924	0.681	0.653	0.792	0.633
	SE	0.731	0.697	0.901	0.731	0.843	0.892	0.660	0.941	0.712	0.615	0.808	0.566
	SEU	0.742	0.681	0.907	0.732	0.873	0.092	0.688	0.056	0.734	0.466	0.799	0.492
	SelfCheckGPT	0.797	0.752	0.917	0.782	0.816	0.888	0.619	0.950	0.659	0.674	<b>0.812</b>	0.667
	<i>P</i> (True)	<b>0.921</b>	0.749	<b>0.932</b>	0.745	<b>0.952</b>	<b>0.951</b>	<b>0.836</b>	<b>0.979</b>	0.677	0.560	0.792	0.542
	Logistic	0.795	<b>0.914</b>	0.905	0.934	0.901	0.906	0.744	0.932	0.767	0.780	0.791	0.795
Qwen3-14B	HaluNet (Ours)	<b>0.810</b>	<b>0.933</b>	0.909	<b>0.952</b>	<b>0.922</b>	<b>0.951</b>	<b>0.777</b>	<b>0.960</b>	<b>0.779</b>	<b>0.826</b>	0.793	<b>0.814</b>
	PE	0.787	0.601	0.855	0.636	0.787	0.225	0.611	0.200	0.700	0.578	0.828	0.601
	T-NLL	0.652	0.649	0.851	0.636	0.604	0.363	0.598	0.359	0.624	0.639	0.822	0.634
	EmbVar	0.729	0.663	0.853	0.665	0.796	0.768	0.728	0.812	0.707	0.569	0.822	0.585
	SE	0.766	0.569	0.851	0.584	0.792	0.772	0.750	0.807	0.760	0.599	0.826	0.577
	SEU	0.780	0.557	<b>0.866</b>	0.588	0.820	0.229	0.760	0.172	0.751	0.550	0.837	0.547
	SelfCheckGPT	<b>0.825</b>	0.551	0.851	0.547	0.863	0.810	<b>0.809</b>	0.849	0.771	0.541	0.822	0.524
	<i>P</i> (True)	0.781	0.550	0.851	0.594	<b>0.904</b>	0.863	<b>0.812</b>	0.877	<b>0.808</b>	0.502	0.822	0.527
HaluNet (Ours)	Logistic	0.757	<b>0.866</b>	0.857	<b>0.882</b>	0.844	<b>0.885</b>	0.741	<b>0.899</b>	0.803	<b>0.863</b>	0.846	0.875
	HaluNet (Ours)	0.755	0.822	0.860	0.810	0.894	<b>0.927</b>	0.803	<b>0.933</b>	<b>0.810</b>	<b>0.892</b>	<b>0.855</b>	<b>0.894</b>

On Llama3-8B, HaluNet achieves **AUROC 0.839, F1@B 0.532, RA@50 0.965** on SQuAD (full context), improving F1@B by 0.066 and AUROC by 0.067 over the strongest non-trained baseline. On TriviaQA, it attains **AUROC 0.893, F1@B 0.601**, corresponding to gains of 0.066 and 0.144. HaluNet also performs strongly in no-context settings, demonstrating robust hallucination detection regardless of external knowledge. On Qwen3-14B, it achieves state-of-the-art or near-SOTA results across datasets and context conditions.

Regarding efficiency, sampling-based estimators (SE, EmbVar, SEU, Self-CheckGPT) are orders of magnitude slower than single-pass methods such as PE and T-NLL, which are sub-second. However, single-pass methods exhibit lower predictive quality. HaluNet strikes a balance, providing strong detection while maintaining low computational cost, reducing the typical accuracy–cost trade-off in uncertainty-based approaches.

### 4.3 Out-of-Distribution Evaluation

We evaluate HaluNet under OOD settings, with AUROC and RA@50 across train-test splits shown in Fig. 3. As expected, OOD evaluation leads to performance drops: on SQuAD, Llama3-8B decreases by up to 0.037 (CR=0) and 0.113 (CR=1), while Qwen3-14B drops by 0.047 and 0.058. When trained on TriviaQA rather than NQ, Llama3-8B generalizes relatively better on OOD SQuAD. In contrast, Qwen3-14B shows a preference for NQ. Several OOD configurations still exceed the SOTA lines in the figure, highlighting HaluNet’s competitive performance and motivating future work on improving OOD generalization.

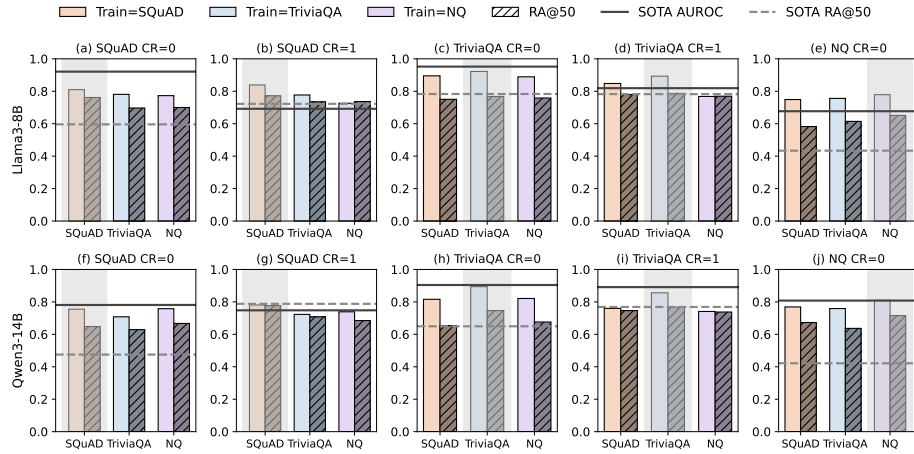


Fig. 3: HaluNet AUROC and RA@50 across training and test sets. Solid and dashed lines indicate AUROC and RA@50 SOTA ( $P(\text{True})$ ), respectively. X-axis: training datasets; Y-axis: metric values; shaded bars mark ID cases.

### 4.4 Ablation Studies

**Impact of Architectural Variants.** We performed an ablation study on HaluNet to assess the contributions of input features, branch encoders, and fusion strategies. Input features included token-level log-likelihood (`ll`), predictive entropy (`ent`), and hidden embeddings (`emb`). Branch encoders were tested in three representative settings: (i) all branches using CNNs, (ii) scalar features (`ll, ent`) with global average pooling + MLP and `emb` with CNN (Fig. 2), and (iii) all branches with global average pooling + MLP. Fusion strategies included attention-based fusion and simple concatenation with MLP. Results under CR=0 are shown in Fig. 4, with similar trends observed under CR=1.

Using all features consistently yields the most robust performance. CNN encoders for all branches with MLP-based fusion often achieve the best or near-best

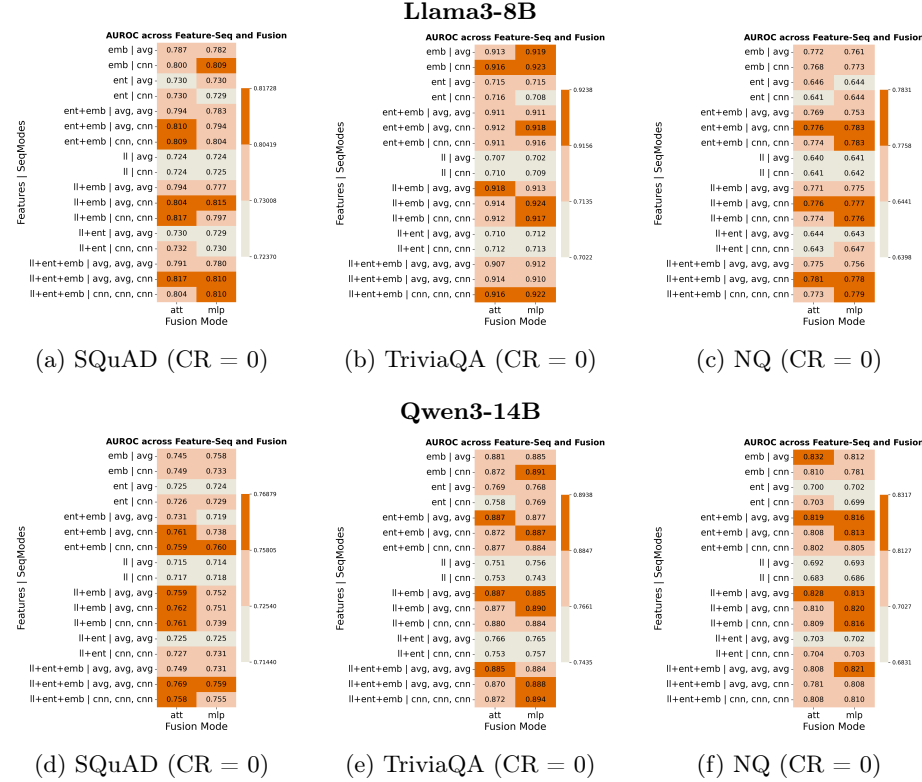


Fig. 4: Heatmap visualization of AUROC achieved by HaluNet under  $\mathbf{CR} = 0$  for different backbone models on SQuAD, TriviaQA, and NQ.

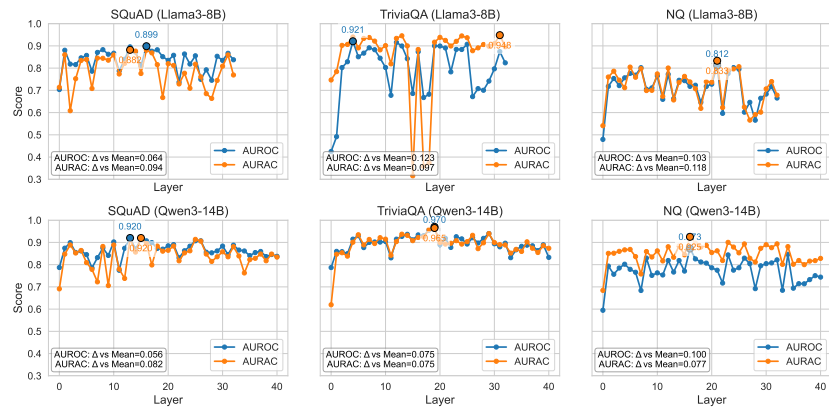


Fig. 5: Layer-wise contribution analysis of hallucination detection performance. The best-performing layer is highlighted, and  $\Delta$  vs Mean denotes the relative improvement of the optimal layer over the average performance.

results. Ablations show that multiple features outperform any single one, with `emb` contributing the largest improvement, while `11` and `ent` provide partially redundant signals. CNNs are particularly effective at capturing local anomalies in `emb`, reflecting both semantic and uncertainty cues, which supports their key role in hallucination detection and suggests potential for disentangling uncertainty signals from embeddings.

**Layer Contribution Analysis.** To evaluate the contribution of hidden representations, we conduct a layer-wise ablation study across backbone models. HaluNet is trained using features from individual transformer layers, and performance is measured in AUROC and AURAC. As shown in Fig. 5, middle layers (typically 8–21) achieve the highest detection accuracy, while bottom layers underperform due to limited semantic abstraction. Higher layers show a slight decline, likely because they specialize in the primary QA task, reducing sensitivity to hallucination-related signals. Although layer 20 is not always the absolute best, it provides stable and reliable performance across models and datasets, so we select it for other experiments.

## 5 Conclusion

We present **HaluNet**, a lightweight framework integrating probabilistic, distributional, and semantic uncertainty signals from single-pass LLM generations. Multi-branch encoders with an adaptive fusion module capture cross-signal interactions, enabling robust and efficient hallucination detection in QA, including out-of-distribution settings. Ablation studies highlight the complementary value of multi-granular features and intermediate-layer embeddings. HaluNet provides a practical, scalable solution for reliable QA hallucination detection, with future work extending to multi-turn and long-form QA scenarios.

## References

1. Aryal, S., Akomoize, M.: Howard university-ai4pc at semeval-2025 task 3: Logit-based supervised token classification for multilingual hallucination span identification using xgbod. In: SemEval. pp. 1790–1794 (2025)
2. Binkowski, J., Janiak, D., Sawczyn, A., Gabrys, B., Kajdanowicz, T.: Hallucination detection in llms using spectral features of attention maps. arXiv preprint arXiv:2502.17598 (2025)
3. Cheung, T.H., Lam, K.M.: Factllama: Optimizing instruction-following language models with external knowledge for automated fact-checking. In: APSIPA ASC. pp. 846–853 (2023)
4. Farquhar, S., Kossen, J., Kuhn, L., Gal, Y.: Detecting hallucinations in large language models using semantic entropy. Nature **630**(8017), 625–630 (2024)
5. Ge, Z., Wu, Y., Chin, D.W.K., Lee, R.K.W., Cao, R.: Resolving conflicting evidence in automated fact-checking: A study on retrieval-augmented llms. arXiv preprint arXiv:2505.17762 (2025)

6. Grewal, Y.S., Bonilla, E.V., Bui, T.D.: Improving uncertainty quantification in large language models via semantic embeddings. arXiv preprint arXiv:2410.22685 (2024)
7. Gu, J., Jiang, X., Shi, Z., Tan, H., Zhai, X., Xu, C., Li, W., Shen, Y., Ma, S., Liu, H., et al.: A survey on llm-as-a-judge. arXiv preprint arXiv:2411.15594 (2024)
8. Guo, J., Wu, Z., Yu, P.S.: Reward inside the model: A lightweight hidden-state reward model for LLM's best-of-n sampling. In: ICML (2025)
9. Hastie, T., Tibshirani, R., Friedman, J., et al.: The elements of statistical learning (2009)
10. Holtzman, A., Buys, J., Du, L., Forbes, M., Choi, Y.: The curious case of neural text degeneration. In: ICLR (2020)
11. Hüllermeier, E., Waegeman, W.: Aleatoric and epistemic uncertainty in machine learning: an introduction to concepts and methods. *Mach. Learn.* **110**, 457 – 506 (2019)
12. Ji, Z., Lee, N., Frieske, R., Yu, T., Su, D., Xu, Y., Ishii, E., Bang, Y.J., Madotto, A., Fung, P.: Survey of hallucination in natural language generation. *ACM Comput. Surv.* **55**(12), 1–38 (2023)
13. Jiang, Z., Araki, J., Ding, H., Neubig, G.: How can we know when language models know? on the calibration of language models for question answering. *TACL* **9**, 962–977 (2021)
14. Joshi, M., Choi, E., Weld, D., Zettlemoyer, L.: TriviaQA: A large scale distantly supervised challenge dataset for reading comprehension. In: Barzilay, R., Kan, M.Y. (eds.) *ACL*. pp. 1601–1611 (2017)
15. Kossen, J., Han, J., Razzak, M., Schut, L., Malik, S., Gal, Y.: Semantic entropy probes: Robust and cheap hallucination detection in llms. arXiv preprint arXiv:2406.15927 (2024)
16. Kwiatkowski, T., Palomaki, J., Redfield, O., Collins, M., Parikh, A., Alberti, C., Epstein, D., Polosukhin, I., Devlin, J., Lee, K., Toutanova, K., Jones, L., Kelcey, M., Chang, M.W., Dai, A.M., Uszkoreit, J., Le, Q., Petrov, S.: Natural questions: A benchmark for question answering research. *TACL* **7**, 452–466 (2019)
17. Liu, L., Pan, Y., Li, X., Chen, G.: Uncertainty estimation and quantification for llms: A simple supervised approach. arXiv preprint arXiv:2404.15993 (2024)
18. Liu, T., Zhang, Y., Brockett, C., Mao, Y., Sui, Z., Chen, W., Dolan, B.: A token-level reference-free hallucination detection benchmark for free-form text generation. In: *ACL*. pp. 6723–6737 (2022)
19. Manakul, P., Liusic, A., Gales, M.: SelfcheckGPT: Zero-resource black-box hallucination detection for generative large language models. In: *EMNLP* (2023)
20. Moslonka, C., Randrianarivo, H., Garnier, A., Malherbe, E.: Learned hallucination detection in black-box llms using token-level entropy production rate. arXiv preprint arXiv:2509.04492 (2025)
21. Quevedo, E., Salazar, J.Y., Koerner, R., Rivas, P., Cerny, T.: Detecting hallucinations in large language model generation: A token probability approach. In: *CSCE*. pp. 154–173 (2024)
22. Rajpurkar, P., Jia, R., Liang, P.: Know what you don't know: Unanswerable questions for SQuAD. In: *ACL*. pp. 784–789 (2018)
23. Reimers, N., Gurevych, I.: Sentence-bert: Sentence embeddings using siamese bert-networks. In: *EMNLP* (2019)
24. Tan, Y., Min, D., Li, Y., Li, W., Hu, N., Chen, Y., Qi, G.: Can chatgpt replace traditional kbqa models? an in-depth analysis of the question answering performance of the gpt llm family. In: *ISWC*. p. 348–367 (2023)

25. Tong, C., Zhang, Q., Jiang, L., Liu, Y., Sun, N., Li, W.: Semantic reformulation entropy for robust hallucination detection in qa tasks. arXiv preprint arXiv:2509.17445 (2025)
26. Wang, K., Duan, F., Wang, S., Li, P., Xian, Y., Yin, C., Rong, W., Xiong, Z.: Knowledge-driven cot: Exploring faithful reasoning in llms for knowledge-intensive question answering. arXiv preprint arXiv:2308.13259 (2023)
27. Yaldiz, D.N., Bakman, Y.F., Buyukates, B., Tao, C., Ramakrishna, A., Dimitriadis, D., Zhao, J., Avestimehr, S.: Do not design, learn: A trainable scoring function for uncertainty estimation in generative LLMs. In: NAACL. pp. 691–713 (2025)
28. Zhang, L., Song, D., Wu, Z., Tian, Y., Zhou, C., Xu, J., Yang, Z., Zhang, S.: Detecting hallucination in large language models through deep internal representation analysis. In: IJCAI. pp. 8357–8365 (8 2025)
29. Zhang, T., Qiu, L., Guo, Q., Deng, C., Zhang, Y., Zhang, Z., Zhou, C., Wang, X., Fu, L.: Enhancing uncertainty-based hallucination detection with stronger focus. In: EMNLP. pp. 915–932 (2023)
30. Zhou, H., Hu, C., Yuan, Y., Cui, Y., Jin, Y., Chen, C., Wu, H., Yuan, D., Jiang, L., Wu, D., et al.: Large language model (llm) for telecommunications: A comprehensive survey on principles, key techniques, and opportunities. IEEE Commun. Surv. Tutor. (2024)